Molecular Crystals and Liquid Crystals
Publication details, including instructions for authors and subscription information:
http://www.tandfonline.com/loi/gmcl16

# Lyotropic Phases from Short Chain Monoalkylphosphate/ Water Systems. A Multinuclear NMR and X Ray Diffraction Study

B. Perly [a] , J. P. Quaegebeur [a] , C. Chachaty [a] & B. Gallot [b]

[a] Département de Physico-Chimie, Centre d'Edudes Nucléaires de Saclay, F. 91191 GIF SURYVETTE, CEDEX, France

[b] Centre de Biophysique Moléculaire, 1A Avenue de la Recherche Scientifique, F. 45045 ORLEANS, CEDEX, France

Version of record first published: 20 Apr 2011.

To cite this article: B. Perly , J. P. Quaegebeur , C. Chachaty & B. Gallot (1985): Lyotropic Phases from Short Chain Monoalkylphosphate/ Water Systems. A Multinuclear NMR and X Ray Diffraction Study, Molecular Crystals and Liquid Crystals, 128:3-4, 287-304

To link to this article: http://dx.doi.org/10.1080/00268948508079497

*Mol. Cryst. Liq. Cryst.*, 1985, Vol. 128, pp. 287–304
0026-8941/85/1284–0287/$20.00/0

Printed in the United States of America



# Lyotropic Phases from Short Chain Monoalkylphosphate/Water Systems. A Multinuclear NMR and X Ray Diffraction Study

B. PERLY, J. P. QUAEGEBEUR and C. CHACHATY

*Département de Physico-Chimie, Centre d'Etudes Nucléaires de Saclay, F. 91191 GIF SUR YVETTE CEDEX (France)*

and

B. GALLOT

*Centre de Biophysique Moléculaire, 1A Avenue de la Recherche Scientifique, F.45045 ORLEANS CEDEX (France)*

(*Received May 15, 1984; in final form July 20, 1984*)

The phase diagrams of sodium monobutyl and monohexyl phosphate/water systems have been derived from NMR and X-Ray diffraction experiments. Isotropic, lamellar, hexagonal and gel phases have been observed over the considered concentration and temperature range (surfactant molar fraction $X_M$ from 0.1 to 0.4 and $-20°C < T < 100°C$). They were delineated by $^{31}P$ and water $^{2}H$ NMR and identified by means of small angle X ray diffraction from which geometrical parameters have been derived. The hexagonal phase was shown to exhibit a strong tendency to orient in the magnetic field upon slow cooling from the isotropic phase. This macroscopic orientation remains indefinitely stable out of the magnetic field. Monobutyl and monohexyl phosphates exhibit similar phase diagrams which can be derived from each other by a simple shift along the concentration and temperature scales. Only the monobutyl derivative has therefore been extensively studied. Special attention has been paid to the hexagonal phase, since its orientation properties allow some particular experiments to be done. $^{2}H$ NMR was used to monitor the orientation of water molecules in the hexagonal phase. The molecular order and equilibrium conformation of the surfactant molecules were derived from $^{31}P$ chemical shift anisotropy, $^{2}H$ quadrupolar splittings of the hydrocarbon chain, as well as by means of the unusually well resolved $^{13}C - ^{31}P$ and $^{1}H - ^{31}P$ dipolar couplings observed on oriented samples.

## INTRODUCTION

Surfactant molecules containing both an aliphatic chain (hydrophobic core) and a polar head group give rise generally to lyotropic liquid crystalline phases upon mixing with appropriate amounts of water. A very large number of such compounds have been studied[1] because of their practical interest. However, since their properties are primarily due to the amphiphilic character, much attention has been given to surfactant molecules containing long hydrocarbon chains (from 8 to 18 carbon atoms). A complete determination of molecular order along the chain (using essentially $^2H$ NMR) is very difficult if selective deuteration is required to make unequivocal analysis. Moreover, computer simulation of molecular conformations quickly becomes impossible for an increasing number of carbon atoms, since overwhelmingly large memory sizes and computing times are required. It is therefore of interest to seek for chemically simpler models. In a previous study, we have shown[2] that in a given concentration-temperature range, sodium dibutyl phosphate-water systems exhibit a stable lamellar phase. We now report some results obtained with even simpler molecules, i.e., the monosodium salts of monohexyl and monobutyl phosphoric acids. In spite of their limited chain lengths, these systems are shown to exhibit a variety of lyotropic phases upon mixing with water. Most of the data presented here deal with sodium monobutyl hydrogenophosphate. Results with the monohexyl derivative are very similar and only the phase diagrams will be compared.

## EXPERIMENTAL

Monoalkyl phosphoric acids have been prepared from the corresponding alcohols and $POCl_3$ using published procedures.[3] Perdeuteriated *n*-butanol, $^2H_2O$, $^1H_2O$ and $^2H_2{}^{17}O$ where from CEA (Saclay, France). [1.1 $^2H_2$] and [1.1.2.2. $^2H_4$] butanols were obtained by $LiAl^2H_4$ reduction of normal and [2.2.2′.2′ $^2H_4$] butyric anhydrides respectively. The latter compound was previously[4] obtained by decarboxylation of $^2H_2O$ exchanged ethylmalonic acid. All samples were found to be at least 98% pure by $^{31}P$, $^{13}C$ and $^1H$ NMR using dilute solutions in $^2H_2O$. The free monobutyl ($MBPH_2$) and monohexyl ($MHPH_2$) phosphoric acids were converted into the monosodium salts (MBPHNa and MHPHNa) by adjustment to pH = 5.2 of a dilute aqueous solution with NaOH. Further treatment with active charcoal, Chelex 100 chelating resin and final filtration on 0.45 $\mu$

Millipore filters yielded a clear colorless solution. The pure monosodium salts were obtained upon freeze-drying as white fluffy hygroscopic powders.

Depending on the kind of NMR experiments, samples were either prepared in $^2H_2O$ or in deuterium depleted $^1H_2O$. The solid salts were weighted in 8 mm OD glass tubes. After addition of the required amount of water, the tubes were frozen and sealed under vacuum. Visually homogeneous samples were obtained after heating at 60–70°C for periods of time ranging from a few minutes to several hours depending upon the concentration of water. Samples of low water content were obtained preferably by slowly concentrating dilute solutions.

NMR measurements have been performed using either a Bruker WM 500 multinuclear spectrometer (superconducting magnet, $B_0 = 11.74T$) or an iron core WH 90 Bruker multinuclear spectrometer ($B_0 = 2.17T$). Single pulse experiments have been used in all cases. All samples were allowed to reach thermal equilibrium for at least 15 min after any temperature change.

The NMR samples have been further analysed by small angle X-ray diffraction using a Guinier type chamber. The system was maintained under high vacuum, the sample being sealed between Mylar windows in aluminium cells. A bent quartz monochromator was used to focus the 1.54 Å copper radiation along a vertical line. The sample was heated using an electrical oven, the temperature being controlled to $\pm 0.5$°C. Characteristic parameters have been measured directly on the photographic film and the reported data have an estimated precision of $\pm 0.5$ Å.

## RESULTS

### I. $^{31}$P NMR observation of lyotropic phases

$^{31}$P NMR was first used to examine the behaviour of monoalkylphosphate/water systems as a function of temperature and concentration. Throughout this paper, concentration will be given as the molar fraction of surfactant in the sample ($X_M$). This parameter is preferred to the classical percent weight, since it allows direct comparison between samples prepared in $^1H_2O$ or $^2H_2O$, although small isotopic effects have been detected. Experiments in progress show that the isotropic phase corresponds to a micellar solution containing a large amount of monomeric species. The $^{31}$P spectra of the lamellar ($L_\alpha$) and hexagonal ($H_I$) phases are characteristic of axially symmet-

ric systems. Going from the hexagonal to the lamellar systems is evidenced by the simultaneous inversion and increase of the chemical shift anisotropy. The position of the hexagonal phase in the phase diagram (*vide infra*) strongly supports the $H_I$ type, formed of long cylinders the cores of which contain the hydrophobic aliphatic chains.

## II. $^2$H NMR of water molecules in the mesophases

A further confirmation of the results of $^{31}$P experiments was provided by water $^2$H spectra. Figure 1 shows some spectra typical of the phases. The "gel" phase is characterized by a marked line-broadening indicative of a restricted motion of both water and surfactant molecules. It probably corresponds to rigid surfactant surrounded by water molecules incorporated in the lattice. No isotropic line has been observed in the vicinity of 0°C, below the transitions with the $H_I$ and $L_\alpha$ phases, in contrast with the sodium dibutylphosphate/water system under similar conditions, where we are probably dealing with a mixture of ice and organic crystals. In Figure 2, the shaded area

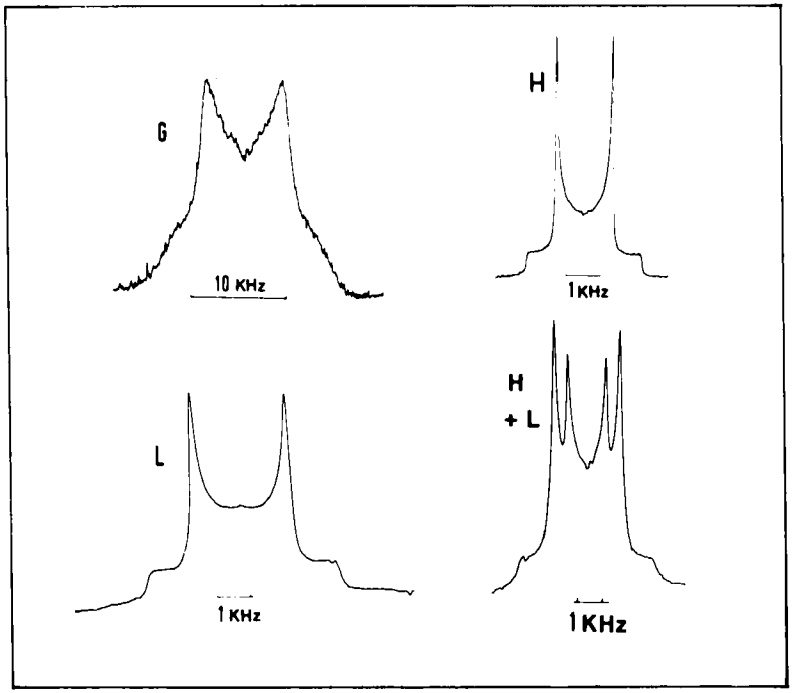


FIGURE 1 $^2$H NMR spectra of $^2H_2O$ in MBPHNa/$^2H_2O$ systems. $H_1$ = direct hexagonal phase ($X_M$ = 0.17, 300 K). $L_\alpha$ Lamellar ($X_M$ = 0.40, 300 K) $H_1 + L_\alpha$($X_M$ = 0.22, 300 K). G = gel phase ($X_M$ = 0.40, 270 K).

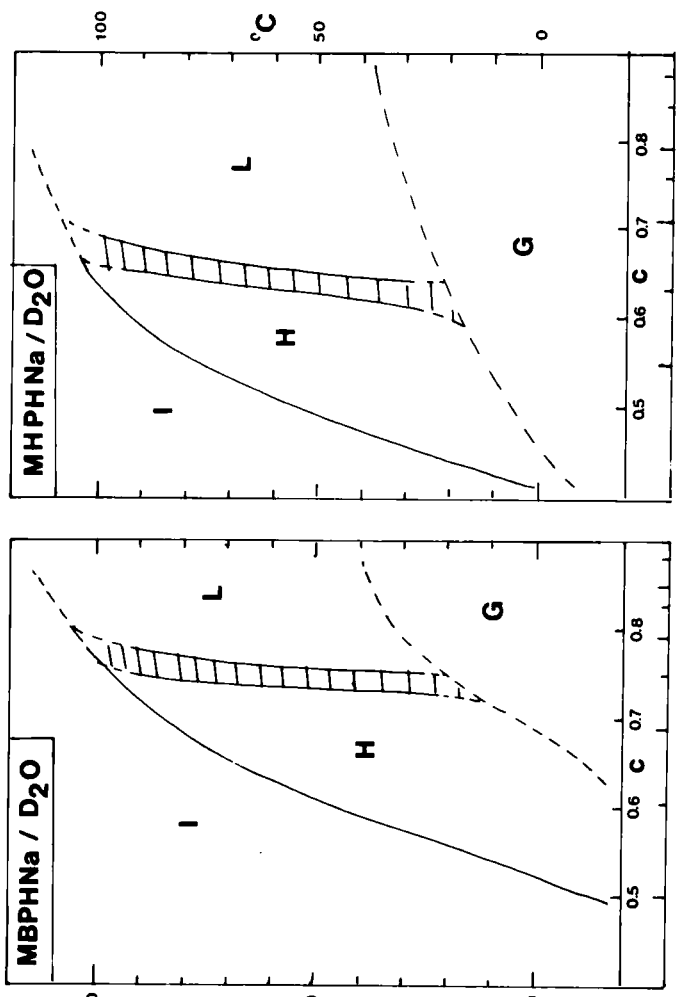


FIGURE 2 Phase diagrams of sodium monobutyl (A) and sodium monohexyl (B) hydrogenophosphates/-water systems. $X_M$ and $C$ are the molar fraction and weight % of surfactant respectively. For the monobutyl derivatives this diagram was built using $^{31}P$ and $^{2}H$ NMR at $C = 0, 55, 0, 60, 0.65, 0.70, 0.72, 0.74, 0.766, 0.78, 0.80$ and 0.82, X-ray experiments being run with $C = 0.65, 0.70, 0.80$ and 0.82.

corresponds to a region where two $^2H$ quadrupolar patterns related to the $H_I + L_\alpha$ mixture are superimposed.

### III. Phase diagrams and X-ray diffraction

Temperature dependence studies of the $^2H$ and $^{31}P$ NMR parameters allowed us to describe the whole phase diagram in the range $-20$ to 100°C. Studies at higher temperatures were precluded by hydrolysis of the samples observed upon heating at 100°C for periods of time exceeding one hour. The complete phase diagrams of MBPHNa and MHPHNa are shown in Figure 2. In the G phase, partial organization of the aliphatic chains was observed by X-ray diffraction, since large angle lines appeared under these conditions. However, this organization of the chains does not seem to be highly cooperative as expected for these very short chain lengths. The temperature range of the $L_\alpha \rightarrow$ G transition is *ca.* 10°C. The nature of the hexagonal phase first identified by $^{31}P$ NMR was further confirmed by X-ray diffraction, since three diffraction orders have been detected in the expected[5] ratio 1, $\sqrt{3}$, 2. The hexagonal to isotropic transition was found to occur at the same temperature as that obtained by NMR analysis. The complete disappearance of diffraction lines in this phase supports the isotropic (micellar) structure and is not consistent with other symmetric phases (i.e., cubic systems) which are magnetically isotropic. The lamellar phase ($L_\alpha$) was shown by X-ray diffraction to give rise to two or three identically spaced diffraction lines. An expected "melting" of the $L_\alpha$ phase to an isotropic structure at high temperature could not be detected since degradation was very fast at $T > 100$°C. It is clear from Figure 2 that the phase diagrams of monobutyl and monohexyl phosphates are derived from each other by a simple translation along the temperature and concentration scales. Most of the data presented in this paper will therefore deal with the simpler monobutyl derivative. In both cases, the limit between $L_\alpha$ and $H_I$ phases is almost vertical and no thermal transition could be induced between these phases. On the other hand, the hexagonal to isotropic phase transition occurs in a very narrow temperature range. Temperature cycles could be repeated many times along this transition without any detectable hysteresis. The temperature dependence of the NMR parameters have been studied and will be compared to the geometrical parameter dependence in the next section of this paper.

### IV. Geometrical parameters of the $L_\alpha$ and $H_I$ phases of MBPHNa

X-ray diffraction experiments yield only the total layer thickness $d_t$ and the distance $d$ between the axes of cylinders for the lamellar and

hexagonal phases respectively. Simple geometrical considerations however allow the respective contributions of the polar and aliphatic parts to be determined.[5]

For the hexagonal phase, the area per polar head $S$ and the diameter $2R$ of the cylinders containing only the aliphatic chains are given by the following equations:

$$S = \frac{2M_B\bar{V}_B}{Nd} \cdot \frac{2\pi}{\sqrt{3}} \cdot \left[ 1 + \frac{X_A\bar{V}_A}{X_B\bar{V}_B} + \frac{(1-C)\cdot\bar{V}_S}{C\bar{V}_B} \right] \quad (1)$$

$$R = \frac{2M_B\bar{V}_B}{NS} \quad (2)$$

with

$C$: Surfactant concentration in the sample (weight ratio)
$X_A, X_B$: weight ratio of the polar and non-polar moieties of the surfactant molecule.
$\bar{V}_A, \bar{V}_B$: specific volumes of the polar and non-polar moieties
$V_S$: specific volume of the solvent
$M_B$: molecular weight of the aliphatic chain
$N$: Avogadro number.

The specific volume of the surfactant (MBPHNa) was measured by pycnometry ($V_{AB} = 0.68\ cm^3 \cdot g^{-1}$). $\bar{V}_A$ and $\bar{V}_B$ where derived assuming additivity of partial molar volumes. This yields $\bar{V}_A = 0.31\ cm^3 \cdot g^{-1}$ and $\bar{V}_B = 1.423\ cm^3 \cdot g^{-1}$, using the literature data for the molar specific volumes of $CH_2$ (16.3 $cm^3$) and $CH_3$ (32.15 $cm^3$) units.[6] The obtained values of $S$ and $2R$ for the hexagonal phase are shown in Figure 3. It is observed that they are almost temperature independent in the range considered here. For the monobutyl derivative, typical values are $S = 66\ Å^2$ and $2R = 8.2$ Å for $C = 0.65$.

Similar relations can be derived for the lamellar phase from the total layer thickness $d_t$. The ratio of the two sublayers thicknesses ($d_A, d_B$, thickness of the polar and aliphatic layers respectively) and the average area per polar head are given by:

$$d_B/d_A = \frac{CX_B\bar{V}_B}{CX_A\bar{V}_A + (1-C)\bar{V}_S} \quad (3)$$

$$S = \frac{2M_B\bar{V}_B}{Nd_t} \left[ 1 + \frac{X_A\bar{V}_A}{X_B\bar{V}_B} + \frac{(1-C)\bar{V}_S}{CX_B\bar{V}_B} \right] \quad (4)$$

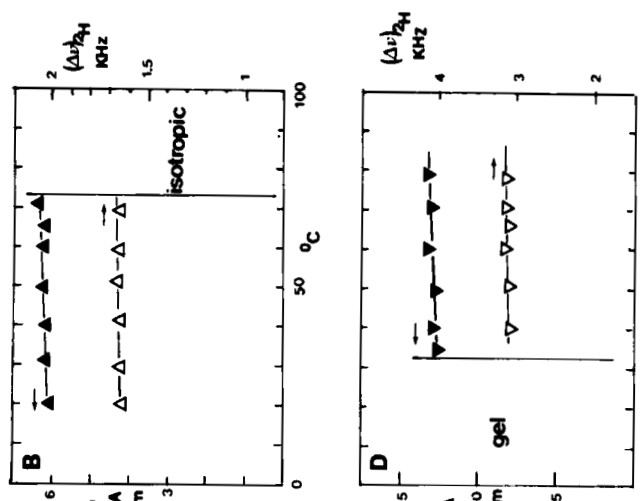


FIGURE 3 Temperature dependence of lattice and NMR parameters for liquid crystalline phases of MBPHNa/$D_2O$. A, B: Hexagonal phase ($X_M = 0.14$). Temperature dependence of the distance between centers of rods (○), diameter $2R$ of the cylinders containing the aliphatic chains (●), average area per polar head (•), $^{31}P$ chemical shift anisotropy (▲) and $^2H$ quadrupolar splittings from $^2H_2O$(△). C, D: Lamellar phase ($X_M = 0.40$). Temperature dependence of the total layer thickness $d_t$(■) and the aliphatic layer (□), average area per polar head at interface (•), $^{31}P$ chemical shift anisotropy (▼) and the $^2H$ quadrupolar splittings from $^2H_2O$(▽).

For $C = 0.8$, typical values are $S = 25$ Å$^2$, $d_A = 9.3$ Å and $d_B = 10$ Å. They are almost temperature independent as shown in Figure 3. The constancy of all geometrical parameters in the considered temperature range for pure phases is consistent with the observation that NMR parameters (shown in the same figure) do not experience any significant variation under the same conditions.

For MBPHNa, the transition from the lamellar to the hexagonal phase involves, as expected, a significant increase in the available area per polar head and a reduction of the average aliphatic chain length.

## V. Orientation of the hexagonal phase in the magnetic field

The orientation properties of the hexagonal phase under study is evidenced by NMR on all observed nuclei. NMR observation of freshly prepared samples shows typical polycrystalline powder spectra with axial symmetry (see for example the $H_I$ type spectra in Figures 4*a* and 5*a*). However, if the sample is heated in the spectrometer probe up to the pure isotropic phase and slowly cooled down, typical oriented spectra are obtained. Full thermal cycles are shown in Figures 4 and 5. This behaviour is characteristic of the macroscopic orientation of the directors in the magnetic field. In the present case, the long rods of the hexagonal phase are on the average parallel to the static magnetic field. In fact, the line shapes are characteristic of an orientation distribution about this direction. This macroscopic orientation is frozen out if the sample temperature is lower than the hexagonal to isotropic transition. No disruption takes place if the sample is removed from the magnetic field, and the macroscopic orientation remains unchanged after several months at room temperature. This outstanding feature is further shown in Figure 6 where different combinations of orienting-observing fields have been considered. It is clear, however, that a more perfect orientation is achieved at very high field (11.74$T$) since sharper and more symmetrical lines are observed as compared to medium field spectrometers (2.11$T$). This property makes it possible to obtain very well resolved spectra as shown in Figure 7. The angular dependence of the $^2$H splittings and line-shapes observed at 2.17$T$, where the sample tube is oriented perpendicular to $H_0$, have been interpreted by a narrow orientation distribution of the rods in a plane orthogonal to the sample axis (Figure 8), which may be approximated by a gaussian function of *ca.* 15° half-width. No very significant differences were observed between 5 mm and 10 mm o.d. samples, showing that the wall effect is not the predominant factor of this distribution.

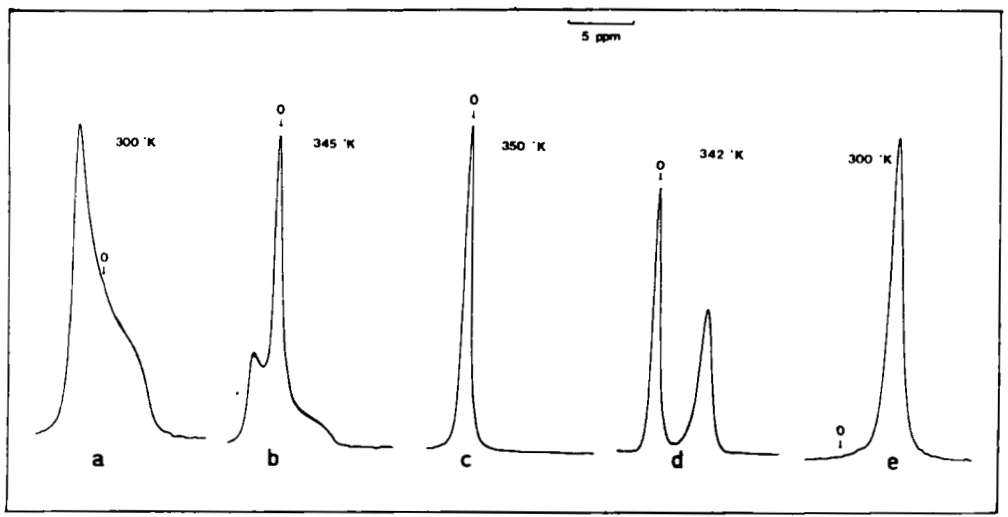


FIGURE 4 $^{31}P$ NMR evidence for the orientation of the hexagonal phase and for a thermally-induced hexagonal-isotropic-hexagonal transition. The arrows indicate the isotropic chemical shift position. Sample: MBPHNa/$^{2}H_2O$ $X_M = 0.17$.

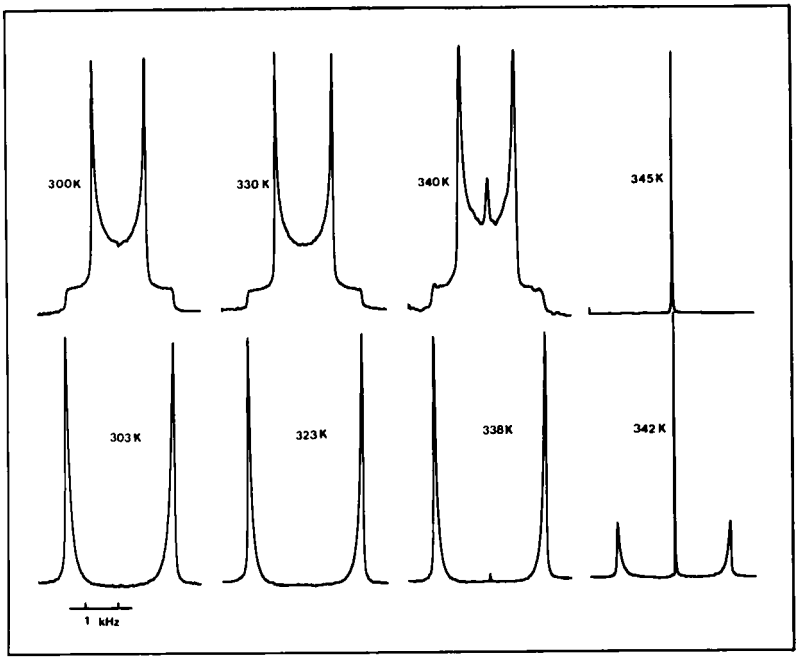


FIGURE 5 Temperature dependence of the water deuteron NMR spectra in the hexagonal phase of MBPHNa/$^2H_2O$. Parameters are identical to Figure 4.

## VI. Molecular order and conformation of the surfactant molecules in the MBPHNa/water hexagonal phase

The $^{31}P$ chemical shift anisotropy (CSA), the deuterium quadrupolar splittings of the hydrocarbon chain, as well as the unusually well resolved $^{13}C-{}^{31}P$ and $^{31}P-{}^{1}H$ dipolar splittings in oriented samples allow a conformational analysis of MBPHNa in the hexagonal phase. This analysis was performed by using the geometrical parameters[7] of the

$$-CH_2-O-\underset{O^-}{\overset{P}{|}}(O)-OH$$

residue. The molecular axes used in the present study are given in Figure 9. The principal values of the CSA tensor are taken as a mean of those given in[8] with $\sigma_{11} = -56$ ppm, $\sigma_{22} = -2$ ppm along the $O_1O_2$ direction and the bisector of $O_3PO_4$ respectively, and $\sigma_{33} = +58$ ppm. $^2H$ and $^{17}O$ NMR experiments on water nuclei show that the ratio of the $^{17}O/^2H$ quadrupolar splittings is nearly 3 instead of *ca.* 6 for other

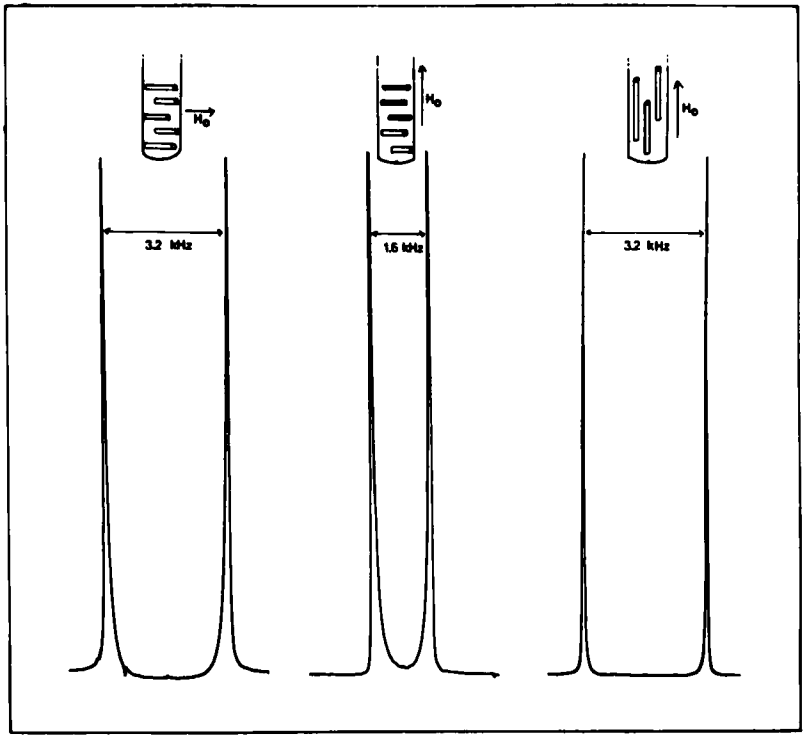


FIGURE 6 $^{2}H$ NMR spectra of oriented samples of MBPHNa/$^{2}H_2O$ in the hexagonal phase, using different combinations of field and macroscopic orientation directions. The vertical (relative to the sample tube) and horizontal fields are generated by the WM 500 and WH 90 spectrometers respectively (see experimental section).

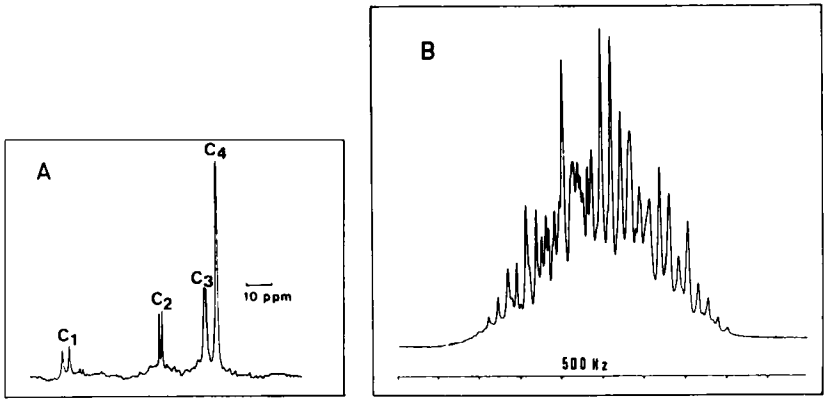


FIGURE 7 "High resolution" $^{13}C$ (A) and undecoupled $^{31}P$ (B) NMR spectra (11.74 *T*) of an oriented hexagonal sample (MBPHNa/$^{2}H_2O$ $X_M = 0.17$, 300 K).

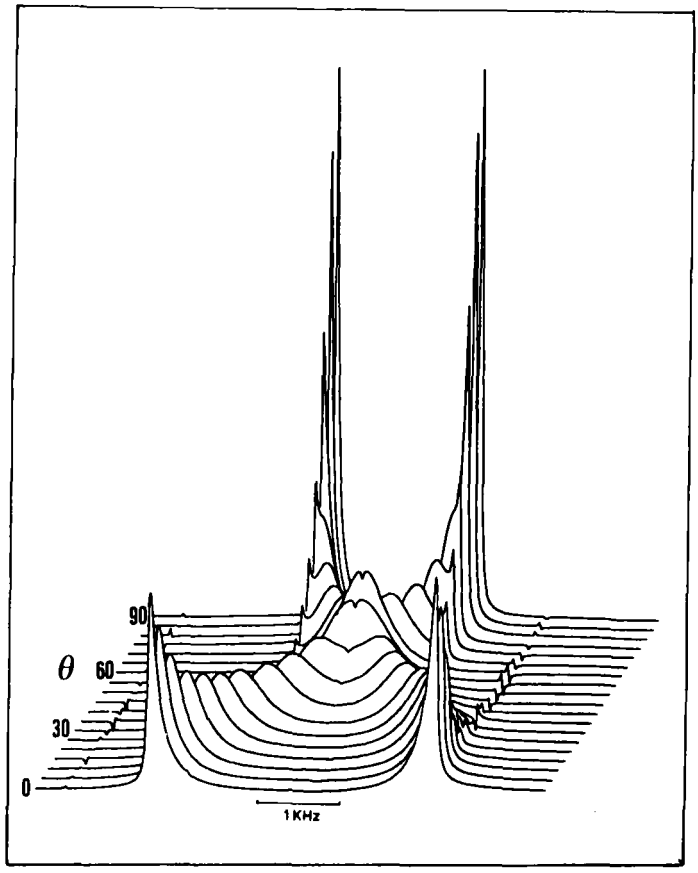


FIGURE 8 Angular dependence of $^2H$ (from $^2H_2O$) quadrupolar splittings and line shape obtained by rotating an oriented hexagonal sample in the magnetic field (MBPHNa/$^2H_2O$, $X_M = 0.172$, 300 K, 13.8 MHz).

lyotropic systems, in particular the dibutyl phosphate/water $L_\alpha$ phase.[2] This result suggests a fast exchange between the hydroxylic or deuteron proton of the phosphate group and water and, therefore, among the three equivalent oxygens of this group. This exchange averages the CSA tensor along the $P - O_1$ direction with:

$$\sigma = \sigma_{11}\cos^2\Phi \sin^2\theta + \sigma_{22}\sin^2\Phi \sin^2\theta + \sigma_{33}\cos^2\theta \qquad (5)$$

$\theta = 90°$, $\Phi = 35°$ being the polar and azimuthal angles of $P \overrightarrow{-} O_1$ in the principal axes of the $\boldsymbol{\sigma}$ tensor. One finds thus $\sigma_{\parallel} \simeq -38$ ppm and $\sigma_{\perp} = 19$ ppm. The observed chemical shift-anisotropy expressed in

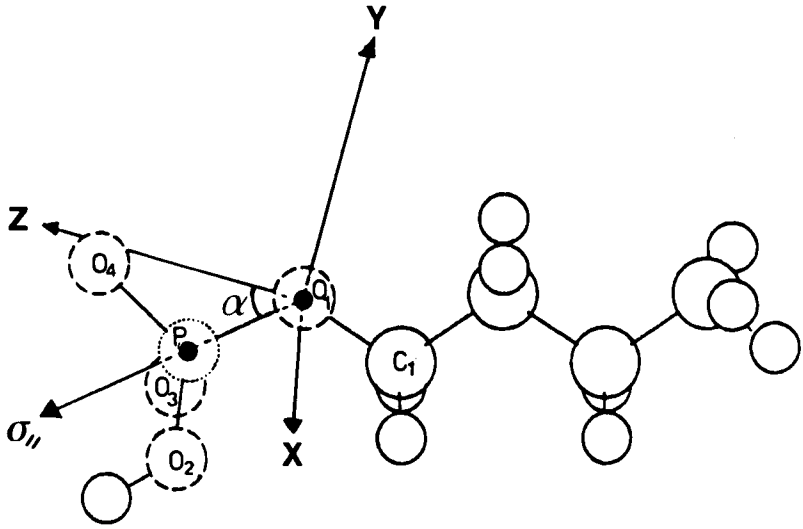


FIGURE 9 Monobutyl phosphate in the all-*trans*-conformation. $\sigma_{\parallel}$ and X, Y, Z denote the symmetry axis of the exchange-averaged C.S.A. tensor and the molecular reference frame, respectively.

ppm being independent of the magnetic field ($H_0 = 2.11T$ and $11.74T$), the exchange rate is likely to be much larger than $\omega_P \times (\frac{3}{2}\sigma_{33} - (\sigma_{\parallel} - \sigma_{\perp})) \simeq 4 \times 10^4\ s^{-1}$, $\omega_p$ being the $^{31}P$ Larmor frequency for $H_0 = 11.75T$.

In a hydrocarbon chain, the deuteron quadrupolar tensor is axially symmetric about the C – D bond, the coupling constant being[9] $\chi_q = e^2qQ/h \simeq 170$ KHz, and is further averaged by the overall motion of the molecule as well as by the *trans-gauche* isomerization. The deuteron quadrupolar splittings $\Delta\nu_i$ are given[10] by the expression:

$$(\Delta\nu_i)_{^2H} = \tfrac{3}{8}(3\cos^2\Psi - 1)\chi_q \times \left[\langle 3l_{z_iZ}^2 - 1\rangle S_{ZZ} + (S_{XX} - S_{YY})\langle l_{z_iX}^2 - l_{z_iY}^2\rangle\right] \quad (6)$$

For the $^{13}C - ^{31}P$ and $^{31}P - ^{1}H$ dipolar splittings and $^{31}P$ chemical shift anisotropy, we have likewise:

$$(\Delta\nu_i)_{dip} = \frac{\gamma_i\gamma_P h}{8\pi^2}(3\cos^2\Psi - 1)\left[\langle(3l_{z_iZ}^2 - 1)r_i^{-3}\rangle S_{ZZ} + (S_{XX} - S_{YY}) \times \langle(l_{z_iX}^2 - l_{z_iY}^2)r_i^{-3}\rangle\right] \quad (7)$$

$$(\Delta\sigma)_{^{31}P} = \frac{3}{4}\sigma_{\parallel}\left[(3l_{zZ}^2 - 1)S_{ZZ} + (S_{XX} - S_{YY})(l_{zX}^2 - l_{zY}^2)\right] \quad (8)$$

In these equations, $\Psi$ is the angle between the static magnetic field and the director of the mesophase, $S_{XX}, S_{YY}, S_{ZZ}$ are the molecular order parameters, $l_{zX}, l_{zY}, l_{zZ}$ denote the direction cosines of the symmetry axes of the magnetic tensor with the principal direction of the ordering tensor, and $r_i$ is the time dependent $C_i - P$ internuclear distance.

Because of the symmetries of the molecule, we assume that the $Y$ and $Z$ axes are in the $P - O_1 - C_1$ plane. The angle $\alpha$ of the $Z$ axis with $P - O_1$ is an adjustable parameter. In Equations 6–8, the angular brackets correspond to a statistical average over the 27 possible conformations of the $P - O - C - C - C - C$ fragment which depends upon the populations of the *trans*-(T) and *gauche*-($G^{\pm}$) rotamers about the $O_1 - C_1$, $C_1 - C_2$ and $C_2 - C_3$ bonds. The statistical weight of a given molecular conformation $u$ may be expressed by its total potential energy with respect to the all-*trans* form:

$$P_u = \frac{\exp\left(-\frac{E_u}{RT}\right)}{\sum_u \exp\left(\frac{-E_u}{RT}\right)} \qquad \text{with} \tag{9}$$

$$E_u = \sum_{j=1}^{3} \delta_j \Delta E_j + \Delta E_{st}, \qquad (\delta_{j_T} = 0, \delta_{j_G} = 1) \tag{10}$$

$\Delta E_j$ being the energy difference between the local *gauche*- and *trans*-forms at the $j$th bond and $\Delta E_{st}$ an increment due to intramolecular steric constraints, such as the occurrence of a $G^+ G^-$ local form.[11]

In micelles and lyotropic phases, the use of Eq. (9) and (10) in the determination of conformational probabilities is questionable because of additional terms associated with the hydration of $CH_2$ or $CH_3$ groups and of the intermolecular constraints due to the close packing of the chains.[12,13] In the systems under study, the quasi-invariance of the relative values of the $^2H$ quadrupolar splittings with temperature, not expected from these equations, suggests that the molecular conformations are governed by intermolecular constraints.

The separation of the intra- and inter-molecular contributions to $\Delta E_j$, being not within the scope of this paper, it seems preferable to denote $P_u$ as a product of the probabilities of the *trans*- and *gauche*-forms about the three central bonds of $P - O - C - C - C - C$, with $P_{G^+} = P_{G^-} = \frac{1}{2}(1 - P_{T_j})$, $P_{T_j}$ being an adjustable parameter. The methyl group is assumed to rotate among three equivalent sites defined by the dihedral angles $\angle C_2C_3C_4{}^2H = 180°, \pm 60°$. The choice of another set of angles such as 270°, ±30° has however a

minor effect on the observed quadrupolar splittings of the methyl deuterons.

Besides the angle $\alpha$, the adjustable parameters of the calculation of the quadrupolar splittings are then the probabilities of the *trans*-rotamers about the $O_1 - C_1$, $C_1 - C_2$ and $C_2 - C_3$ bonds. The order parameters are obtained from the linear system of equations 6 and 8, introducing the experimental values of $(\Delta\nu_i)_{^2H}$ and $(\Delta\sigma)_{^{31}P}$. At 300 K, the best agreement between the observed and calculated values of the quadrupolar and dipolar splittings, as well as of the chemical shift anisotropy, is achieved for $P_T = 0.91$, 0.77, 0.38 about the successive bonds, taking $\alpha = 38°$ (Table I). This set of parameters remains valid in the whole temperature range investigated, as shown on Figure 10. The values of the order parameters show that the $Y$ and $Z$ molecular axes are preferentially oriented along the directions parallel and perpendicular to the axis of the cylindrical rod, respectively.

TABLE I

Experimental and calculated NMR parameters for the MBHP/$H_2O$ hexagonal phase ($T = 300$ K, $X_M = 0.16$).

| | $O - C_1$ | $C_1 - C_2$ | | $C_2 - C_3$ |
|---|---|---|---|---|
| $P_T$[a] | 0.91 | 0.77 | | 0.38 |
| | $H_1$ | $H_2$ | $H_3$ | $H_4$ |
| obs. $\lvert(\Delta\nu)_{^2H}\rvert$ Hz | 15220 | 10520 | 7065 | 2965 |
| calc. | 15690 | 9946 | 7120 | 2591 |
| obs.[d] $\lvert(\Delta\nu)^{P-H}_{dip}\rvert$ Hz | 844 | 361 | 132 | 97 |
| calc. | 840 | 303 | 152 | 107 |
| | $C_1$ | $C_2$ | $C_3$ | $C_4$ |
| obs.[d] $\lvert(\Delta\nu)^{P-C}_{dip}\rvert$ Hz | 342 | 137 | 49 | unresolved |
| calc. | 397 | 118 | 54 | 32 |

| | | obs. | calc. |
|---|---|---|---|
| $(\Delta\sigma)_P$ ppm | | 6.2 | 6.2 |
| | $S_{XX} = 0.084$ | $S_{YY} = 0.257$ | $S_{ZZ} = -0.341$ |

confinment in a cylindrical sector:

| | $O - C_1$ | $C_1 - C_2$ | | $C_2 - C_3$ |
|---|---|---|---|---|
| $P_T$[b] | 0.85 | 0.6 | | 0.6 |
| $P_T$[c] | 0.87 | 0.70 | | 0.36 |
| | $H_1$ | $H_2$ | $H_3$ | $H_4$ |
| $\lvert\Delta\nu_{2_H}\rvert$ calc. | 15730 | 9451 | 8078 | 1463 |

[a] from the best fit of quadrupolar splittings
[b] assumed values for a free chain
[c] resulting from the confinement in a cylindrical sector
[d] the maximum scalar contribution is not expected to be larger than 3%.

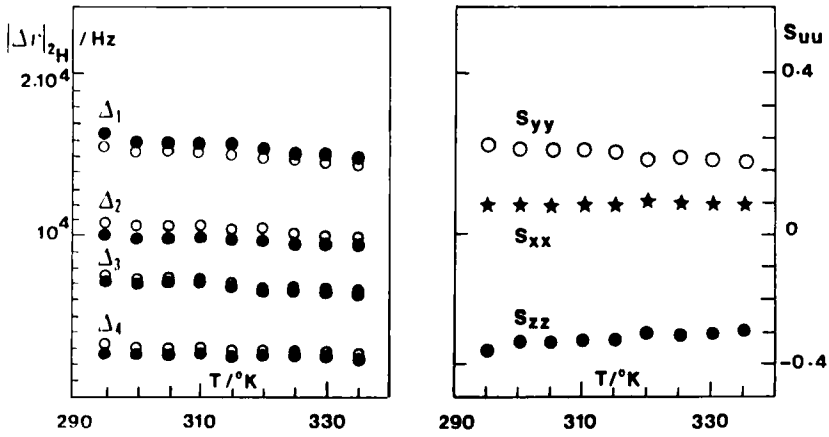


FIGURE 10 Observed (○) and calculated (●) deuteron splittings (left) and molecular order parameters (right) in the MBPHNa/$H_2O$ hexagonal phase.

The effective rotamer populations $P_T$ are quite different from those expected from the $\Delta E_{TG}$ values about the O − C and C − C bonds which are the order of 1000 and 600 cal.mole$^{-1}$ respectively. To explain this difference, we assume that in the hexagonal phase, the MBHP molecule is confined in a cylindrical sector of the rod, the folding back of the chain towards the polar head being prevented by a hard sphere of 2 Å radius surrounding the $^{31}P$ nucleus. For an initial rotamer population $P_T = 0.85$, 0.6, 0.6 about O − $C_1$, $C_1$ − $C_2$ and $C_2$ − $C_3$ assumed for the free molecule, we calculate the effective populations and the quadrupolar splittings by adjusting the area $S$ per polar head assimilated to the square base of the wedge and the radius $R$ of the cylindrical rods. Taking $S = 47$ Å$^2$ and $R = 7.5$ Å, this crude model yields effective rotamer populations and $^2H$ splittings consistent with those resulting from a direct fit of experimental data, except for the methyl group which cannot rotate freely (Table I). Eliminating the sterically-forbidden conformations results in an enhancement of the *trans*-population about O − $C_1$ and $C_1$ − $C_2$ and a decrease of this population about $C_2$ − $C_3$ with respect to the free molecule, as actually observed.

## CONCLUSION

In the present study, we have shown that molecules that are chemically very simple can give rise to the complete phase diagram expected for a binary system, even at fairly high water content. Iso-

tropic, lamellar, hexagonal and "gel" phases have indeed been detected and clearly characterized by multinuclear NMR and small angle X-ray diffraction. From the comparison of monobutyl and monohexyl phosphates, it appears that the chain length is not of considerable importance in the formation of mesophases, but that the nature of the polar head and its hydration properties play a key role. NMR data have been fully confirmed by X-ray diffraction and give very significant information about the local order in the surfactant molecules. Moreover, the orientation properties of the hexagonal phase in the static magnetic field lead to considerable simplification of the spectra and allow important NMR parameters to be measured. Further analysis of molecular order, conformation and dynamics are currently being carried out on these systems. Due to their chemical simplicity, these mesomorphic systems provide very convenient models to investigate the properties of this state of matter and to check theoretical models that are currently available and under development.

## References

1. H. Kelker and R. Hatz, *Handbook of Liquid Crystals* (Verlag Chemie, Basel, 1980), Chap. 11.
2. C. Chachaty and J. P. Quaegebeur, *J. Phys. Chem.* **87**, 4341 (1983).
3. H. R. Gamrath, R. E. Hatton, and W. E. Weesner, *Ind. Eng. Chem.* **46**, 208 (1954).
4. M. E. Isabelle and L. C. Leitch, *Can. J. Chem.* **36**, 440 (1958).
5. B. Gallot, *Adv. Polym. Sci.* **29**, 85 (1978).
6. A. K. Doolittle, *J. Appl. Phys.* **22**, 1471 (1951).
7. J. Kraut, *Acta Cryst.* **14**, 1146 (1961).
8. S. J. Kohler and M. P. Klein, *Biochemistry* **15**, 967 (1976).
9. L. J. Burnett and B. H. Muller, *J. Chem. Phys.* **55**, 5829 (1971).
10. N. Boden, L. D. Clark, R. J. Busby, J. W. Emsley, G. R. Luckhurst, and C. P. Stockley, *Mol. Phys.* **42**, 562 (1981).
11. P. J. Flory, *Statistical Mechanics of Chain Molecules* (Interscience, New York, 1965), Chap. 5.
12. D. W. R. Gruen, *J. Colloïd Interface Sci.* **84**, 281, 1981.
13. K. A. Dill and P. J. Flory, *Proc. Natl. Acad. Sci. USA* **77**, 3115 (1980).